described (19). Immunofluorescence of α-rENaC (7) used a polyclonal antibody against a glutathione-S-transferase fusion protein containing the first 76 amino acids of the NH_2-terminus (29) and CFTR protein-1468 (30), following the protocol of Grubb *et al.* (15). Cells on coated cover slips were fixed in acetone at 20°C for 10 min and incubated in primary antibodies for 90 min at room temperature followed by fluorescein isothiocyanate (FITC)– and Texas Red–conjugated secondary antibodies for 30 min. Parent MDCK cells were used as control. Similar results were obtained for the rENaC subunit.
17. H. H. Ussing, *Physiol. Rev.* **29**, 127 (1949).
18. C. U. Cotton, M. J. Stutts, M. R. Knowles, J. T. Gatzy, R. C. Boucher, *J. Clin. Invest.* **79**, 80 (1987).
19. M. J. Stutts *et al.*, *J. Biol. Chem.* **268**, 20653 (1993).
20. We studied 3T3 cells on the stage of an inverted microscope at 22°C by the techniques of Hamill *et al.* (31). Pipettes were filled with Cl^--free buffer that contained 100 mM Na aspartate, 2 mM $MgSO_4$, 2 mM Na_2ATP, and 5 mM *N*-tris(hydroxymethyl)-methyl-2-aminoethanesulfonic acid (TES) (pH 7.2). Cl^--free extracellular buffer contained 160 mM Na gluconate, 2 mM $MgSO_4$, 1 mM $CaSO_4$, and 5 mM TES (pH 7.2). [See (32) for other details.] Solutions containing amiloride (final concentration 10^{-5} M) and cpt-cAMP (5×10^{-4} M)/forskolin (1×10^{-5} M) were added by a 1:2 dilution of the extracellular bath.
21. Swiss 3T3 fibroblasts stably expressing the human CFTR gene (32) or an inactive interleukin-2 receptor (33) were infected with a retrovirus expression vector encoding the α-, β-, and γ-rENaC subunits. The three subunits were expressed from the viral long terminal repeat on a tricistronic mRNA in the order (5′ to 3′) α, β, γ. Internal ribosomal entry site sequences from encephalomyocarditis virus and poliovirus were included 5′ of the β and γ subunit sequences, respectively, to facilitate translation. Immediately 3′ to the γ subunit, an SV40 promoter was included to drive transcription of a puromycin-selectable marker. Fibroblasts were exposed to virus (10^2 CFU/ml) in polybrene (8 μg/ml) and were selected in puromycin (1 μg/ml). Resistant colonies were expanded and expression of α-, β-, and γ-rENaC subunits was determined by Northern (RNA) blot and protein immunoblot analyses. Immunocytochemistry was as described in Fig. 2.
22. D. A. Ausiello, J. L. Stow, H. F. Cantiello, J. B. de Almeida, D. J. Benos, *J. Biol. Chem.* **267**, 4759 (1992).
23. I. L. Reisin *et al.*, *ibid.* **269**, 20584 (1994); E. M. Schwiebert, T. Flotte, G. R. Cutting, W. B. Guggino, *Am. J. Physiol.* **266**, C1464 (1994).
24. S. Laferte and L. C. Loh, *Biochem. J.* **283**, 193 (1992).
25. R. M. Rios, C. Celati, S. M. Lohmann, M. Bornens, G. Keryer, *EMBO J.* **11**, 1723 (1992).
26. B. Sarkadi *et al.*, *J. Biol. Chem.* **267**, 2087 (1992).
27. N. J. Willumsen, C. W. Davis, R. C. Boucher, *Am. J. Physiol.* **256**, C1033 (1989).
28. B. R. Grubb, R. N. Vick, R. C. Boucher, *ibid.* **266**, C1478 (1994).
29. C. M. Canessa, A. Merillat, B. C. Rossier, *ibid.* **267**, C1682 (1994).
30. J. A. Cohn, O. Melhus, L. J. Page, K. L. Dittrich, S. R. Vigna, *Biochem. Biophys. Res. Commun.* **181**, 36 (1991).
31. O. P. Hamill, A. Marty, E. Neher, B. Sakmann, F. J. Sigworth, *Pfluegers Arch.* **391**, 85 (1981).
32. M. J. Stutts *et al.*, *J. Biol. Chem.* **269**, 8667 (1994).
33. J. C. Olsen *et al.*, *Hum. Gene Ther.* **3**, 253 (1992).
34. We thank P. Blonigen, H. Suchindran, U. S. Rao, and H. Ye for technical contributions and L. Brown for editorial assistance. Supported by NIH grants HL 34322, HL 42384, and CFF R026 and by Swiss National Foundation grant 31-33598.92.

23 February 1995; accepted 19 June 1995

Ultrasound-Mediated Transdermal Protein Delivery

Samir Mitragotri, Daniel Blankschtein,* Robert Langer*

Transdermal drug delivery offers a potential method of drug administration. However, its application has been limited to a few low molecular weight compounds because of the extremely low permeability of human skin. Low-frequency ultrasound was shown to increase the permeability of human skin to many drugs, including high molecular weight proteins, by several orders of magnitude, thus making transdermal administration of these molecules potentially feasible. It was possible to deliver and control therapeutic doses of proteins such as insulin, interferon γ, and erythropoeitin across human skin. Low-frequency ultrasound is thus a potential noninvasive substitute for traditional methods of drug delivery, such as injections.

Transdermal drug delivery (TDD) offers several advantages over traditional delivery methods such as injections and oral administration. Compared to oral delivery, TDD avoids gastrointestinal drug metabolism, reduces elimination by liver, and provides sustained release of drugs for up to 7 days (*1*). Compared to injections, TDD eliminates the associated pain and the possibility of infection. Theoretically, the transdermal route of drug administration could be advantageous in the delivery of many therapeutic proteins because (i) proteins are susceptible to gastrointestinal degradation and exhibit poor gastrointestinal uptake, (ii) proteins such as interferons are cleared rapidly from the blood (*2*) and need to be delivered at a sustained rate in order to be maintained at a high blood concentration, and (iii) transdermal devices are easier to use than injections (*1*).

Despite these advantages, few drugs and no proteins or peptides are currently administered transdermally for clinical applications, because of the low skin permeability to drugs. This low permeability is attributed to the stratum corneum (SC), the outermost skin layer that consists of flat, dead cells filled with keratin fibers (keratinocytes) surrounded by lipid bilayers. The highly ordered structure of the lipid bilayers confers an impermeable character to the SC (*3*). Several methods, which include chemical enhancers (*4*) and electricity (*5*, *6*), have been proposed to enhance transdermal drug transport, but their efficacy has been limited by the large protein size and relatively low electric charge on the proteins.

Application of ultrasound has been attempted to enhance transdermal transport of a few low molecular weight (<500) drugs across human skin (*7*–*10*) as well as proteins such as insulin across animal skin (*11*), a phenomenon referred to as sonophoresis. Although numerous studies of sonophoresis have been performed (*7*–*11*) measurable enhancement has been reported in only a few cases (*8*, *11*). We have shown (*12*) that application of ultrasound at therapeutic frequencies (1 MHz) induces growth and oscillations of air pockets present in the keratinocytes of the SC (a phenomenon known as cavitation). These oscillations disorganize the SC lipid bilayers, thereby enhancing transdermal transport. However, application of therapeutic ultrasound does not induce transdermal transport of high molecular weight proteins. Because cavitational effects are inversely proportional to ultrasound frequency (*13*), we hypothesized that application of ultrasound at frequencies lower than that corresponding to therapeutic ultrasound may induce sufficient bilayer disorganization, so that proteins may be able to diffuse across the skin. We now report that low-frequency ultrasound can induce significant transdermal transport of proteins, including insulin (molecular weight, ~6000), interferon γ (IFN-γ) (~17,000), and erythropoeitin (~48,000).

The passive skin permeability to high molecular weight proteins, including those mentioned above, is essentially zero (below our detection limit). To assess whether application of ultrasound enhances transdermal protein flux, we measured the skin permeability to these proteins in the presence of ultrasound in vitro across human cadaver epidermis (*14*) in a Franz diffusion cell (*15*). In separate experiments, the donor compartment of the diffusion cell was filled with a solution of insulin (100 U/ml), IFN-γ (2500 U/ml), or erythropoeitin (400 U/ml). Ultrasound (20 KHz, 100-ms pulses applied every second) was applied at intensities in the range of 12.5 to 225 mW/cm^2 (*16*) for 4 hours by means of an ultrasound transducer that was immersed in the donor solution. The transducer (area, ~1 cm^2) was oriented perpendicular to, and placed at a distance of 1 cm from, the skin. The concentration of

Department of Chemical Engineering, Massachusetts Institute of Technology, Cambridge, MA 02139, USA.

*To whom correspondence should be addressed.

proteins in the receiver compartment was measured every hour either by radioimmunoassay (RIA) or enzyme-linked immunosorbent assay (ELISA) (*17*). Skin permeabilities to proteins were calculated through use of the transdermal fluxes measured during the first hour (*18*). Ultrasound application induced significant transdermal permeation of insulin (Fig. 1A), IFN-γ, and erythropoeitin. Human skin permeability to insulin at an ultrasound intensity of 225 mW/cm^2 was 3.3×10^{-3} (±35%) cm/hour. The permeability to IFN-γ under similar ultrasound conditions was 8×10^{-4} (±22%) cm/hour, and that to erythropoeitin was 9.8×10^{-6} (±40%) cm/hour (*18*). At these skin permeabilities, it may be possible to deliver these proteins transdermally at a therapeutically relevant rate. For example, one could deliver an insulin dose of about 12 U/hour [a dose given three times a day to a diabetic patient (*19*)] from a transdermal patch with an area of 40 cm^2 (*20*) containing insulin at a concentration of 100 U/ml (*20*). Thus, 1 hour of sonophoresis performed three times a day could deliver the required daily dose of insulin to a diabetic patient. Similarly, an IFN-γ dose of ~5×10^6 U/hour [a daily dose required to enhance the immune response of patients suffering from viral infection or cancer (*21*)] and an erythropoeitin dose of about 140 U/hour [a dose that may be given three times a day to patients suffering from severe anemia (*22*)] may be delivered from a similar patch by application of ultrasound (*20*). The ability of sonophoresis to deliver other macromolecules may be estimated on the basis of their sonophoretic skin permeability, which needs to be measured experimentally (generally decreases with increasing molecular size), and the required therapeutic dose of these macromolecules.

We further analyzed the sonophoretic enhancement of transdermal protein transport by using insulin as a model protein in vitro as well as in vivo. This analysis addresses two issues that are important in the evaluation of ultrasound as a transdermal transport enhancer: (i) the efficacy of low-frequency ultrasound in controlling transdermal flux by varying ultrasound parameters such as the intensity; and (ii) the reversibility of the transdermal transport enhancement, that is, the recovery of the barrier properties of the skin upon turning ultrasound off. The sonophoretic permeability (*18*) varied nearly exponentially with ultrasound intensity (Fig. 1B), probably as a result of a highly nonlinear dependence of cavitation on ultrasound intensity (*23*). Accordingly, ultrasound intensity might potentially be used to control transdermal insulin delivery.

Application of ultrasound under the above conditions did not appear to cause any permanent loss of the barrier properties of the skin. The transdermal insulin flux (proportional to the slope of the curves shown in Fig. 1A) 3 hours after turning the ultrasound off was statistically insignificant. To further assess the recovery of the skin barrier properties after sonophoresis, we measured water transport through the skin

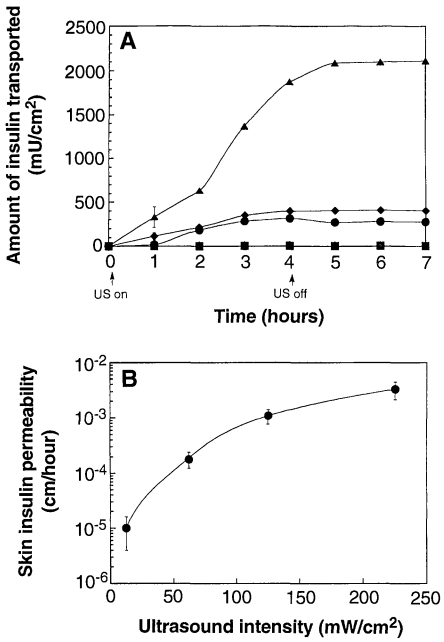

Fig. 1. (**A**) Time variation of the amount of insulin transported across human skin (in vitro) in the presence of ultrasound (20 kHz, 100-ms pulses applied every second) at 12.5 (■), 62.5 (◆), 125 (●), and 225 mW/cm^2 (▲) (n = 3 or 4; error bars, SD). (**B**) Variation of the transdermal insulin permeability (in vitro) with ultrasound intensity (20 kHz, 100-ms pulses applied every second) (n = 3 or 4; error bars, SD). The skin is impermeable to insulin at an ultrasound intensity of 0.

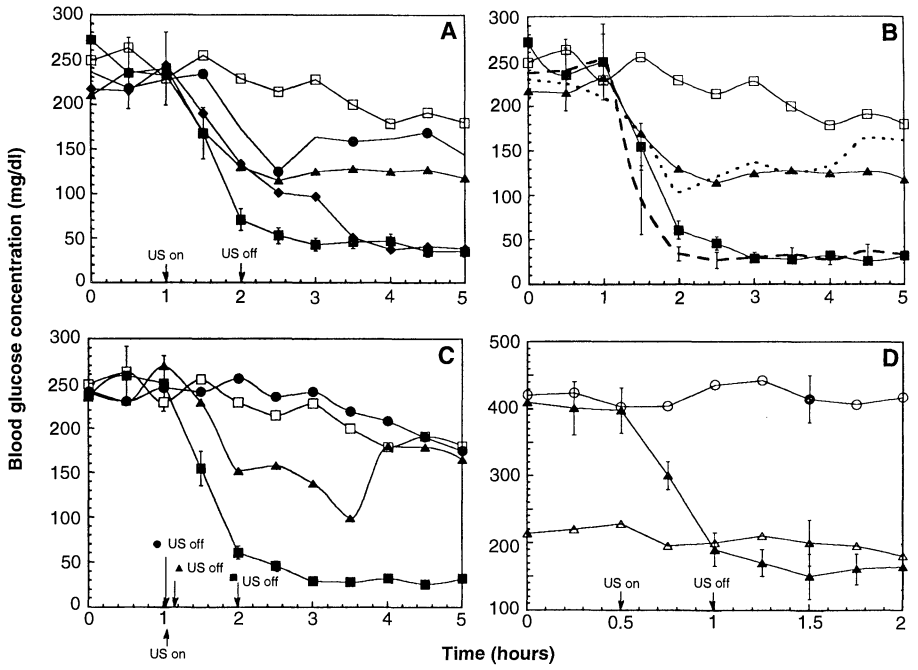

Fig. 2. (**A**) Time variation of blood glucose concentrations of 16-week-old hairless rats (IFFA, Credo, France) upon 1 hour insulin-ultrasound treatment (ultrasound was turned on at 1 hour and turned off at 2 hours) at 12.5 (●) (n = 4), 62.5 (▲) (n = 3), 125 (◆) (n = 3), and 225 mW/cm^2 (■) (n = 5) (30). Control (□), n = 5. Treatment with insulin alone or ultrasound alone did not have any effect on the blood glucose concentration. Error bars (SD) are shown for one set of data. (**B**) Comparison of blood glucose concentration of rats treated for 1 hour (from time 1 to 2 hours) with sonophoresis at 62.5 (▲) (n = 3) and 225 mW/cm^2 (n = 5) (■) and those treated with a single subcutaneous injection at time 1 hour [dashed line, 1 U (n = 3); dotted line, 100 mU (n = 3)]. A typical rat weighed about 400 g. Control (□). Error bars (SD) are shown for one set of subcutaneous and sonophoresis data. (**C**) Time variation of blood glucose concentration of hairless rats exposed to ultrasound (20 kHz, 225 mW/cm^2, 100-ms pulses applied every second) for different times. Ultrasound was turned on at 1 hour and was turned off after 1 min (●) (n = 3), 10 min (▲) (n = 3), and 1 hour (■) (n = 5). Control (□). Error bars (SD) are shown for one set of data. (**D**) Time variation of blood glucose concentration of diabetic hairless rats upon a 30-min insulin-ultrasound treatment (ultrasound was turned on at 0.5 hour and turned off at 1 hour). Diabetes was induced in the hairless rats by injection with streptozotocin (65 mg per kilogram of body weight) and was confirmed by measurements of blood glucose concentration. Sonophoresis was done as described above. Additional blood samples were taken from the tail vein, stored in heparin (~5 μg/ml), and later used to measure plasma insulin concentrations (Linco Research, St. Charles, Montana). Plasma concentration of indigenous rat insulin as well as of delivered human insulin were measured. Diabetic rats (○), normal rats (△), diabetic rats with insulin-ultrasound treatment (▲) (n = 4 per experiment; error bars, SD).

during and after ultrasound exposure (*24*). During sonophoresis, water permeability increased 100-fold, of which about 94 (±3%) was recovered within 2 hours after turning the ultrasound off and 98 (±1%) was recovered within 15 hours. These results suggest that application of ultrasound does not induce any long-lasting loss of the skin barrier properties.

To assess the efficacy of ultrasound in enhancing transdermal flux in an in vivo model, we performed insulin sonophoresis experiments on hairless rats (*25*). An intensity-dependent decrease in the blood glucose concentration was observed upon ultrasound application (Fig. 2A), indicating that low-frequency sonophoresis can effectively deliver intensity-dependent insulin doses across hairless rat skin.

We then estimated the amount of insulin penetrating the hairless rat skin during sonophoresis at various intensities (Fig. 2A). We injected known amounts of insulin in the range of 0 to 1 U subcutaneously (the most common method of insulin administration) into normal rats. The blood glucose concentrations of these rats were then compared with those of the normal rats undergoing sonophoresis. Subcutaneous injection of 100 mU and 1 U of insulin induced a decrease in the blood glucose concentration similar to that induced by sonophoresis at intensities of 62.5 and 225 mW/cm^2, respectively (Fig. 2B). These results suggest that sonophoresis delivers intensity-dependent insulin doses across the skin in the range of approximately 0 to 1 U (through an area of about 3 cm^2).

To estimate the dependence of the amount of insulin delivered on ultrasound exposure time (in vivo), we performed insulin-sonophoresis experiments on normal hairless rats exposed to ultrasound for various times in the range of 1 min to 1 hour. A 1-hour exposure resulted in a decrease of the blood glucose concentration from ~250 to ~30 mg/dl, whereas a 10-min exposure to ultrasound led to a reduction of the blood glucose concentration from about 250 to about 150 mg/dl. This result, compared with the data shown in Fig. 2B, suggests that a 1-hour ultrasound exposure delivers about 1 U of insulin, whereas a 10-min ultrasound application (225 mW/cm^2) delivers about 100 mU through an area of 3 cm^2.

Additional experiments were performed to assess whether application of ultrasound can induce sufficient insulin transport across the skin of a diabetic hairless rat so that its blood glucose concentration becomes comparable to that of normal hairless rats. Insulin-ultrasound treatment reduced the blood glucose concentration of diabetic hairless rats from ~400 to 200 mg/dl (the blood glucose concentration of normal rats) in 30 min (Fig. 2D). A corresponding change in the plasma insulin concentration was observed during sonophoresis. In normal hairless rats, the plasma insulin concentration was 101 ± 31 pM, whereas in diabetic hairless rats it was below the detection limit (34 pM). During sonophoresis performed on diabetic rats, the concentration of transdermally delivered human insulin in rat plasma was 77 (±28) pM after 30 min and 178 (±84) pM after 1 hour. No significant change in the plasma concentration of indigenous rat insulin was observed during sonophoresis.

Initial histological studies were performed to make a preliminary assessment of the safety of low-frequency sonophoresis as a penetration enhancer. These studies (*26*) indicated no physical damage in the skin or in the underlying muscle tissues exposed to ultrasound at all the intensities used in the experiments described above. The regions of hairless rat epidermis exposed to ultrasound were intact. Low-frequency ultrasound has been used safely in clinical applications by dentists for tooth cleaning (*27*). The ultrasound conditions discussed in this report (20 kHz) are similar to those used by dentists (25 to 40 kHz); however, the application time is typically longer in the case of sonophoresis.

Although our preliminary studies indicate no adverse effects of low-frequency ultrasound, further investigation into the safety of low-frequency sonophoresis is required before proceeding with clinical application. Attention should also be focused on the physiological and immunological effects of ultrasound exposure—specifically, whether a change in the method of protein administration from injection to transdermal administration will affect the body's immune response to these proteins. Furthermore, an optimal selection of ultrasound parameters, such as frequency, pulse length, and intensity, and of nonultrasonic parameters, such as ultrasound coupling medium, should be conducted to ensure a safe and efficacious application. With further research, one might envision small, pocket-size sonicators (*28*) carried by the patient to "inject" drugs whenever required. In addition, these devices could potentially be combined with sensors (*29*) that can monitor drug concentrations in the blood to formulate a self-controlled drug (insulin, for example) delivery method that might eliminate the attention required by the patient.

REFERENCES AND NOTES

1. J. J. Elias, in *Percutaneous Absorption: Mechanisms-Methodology-Drug Delivery*, R. L. Bronaugh and H. I. Maibach, Eds. (Dekker, New York, 1989) pp. 1–12. We use "transdermal" as a generic term. However, transport of drugs occurs only across the epidermis where the drug gets absorbed in the blood capillaries.
2. R. M. Frideman, *Interferons: A Primer* (Academic Press, New York, 1981).
3. G. L. Flynn, in (*1*), pp. 27–53.
4. R. R. Burnette, in *Transdermal Drug Delivery: Developmental Issues and Research Initiatives*, J. Hadgraft and R. H. Guy, Eds. (Dekker, New York, 1989), pp. 247–288.
5. M. R. Prausnitz, V. Bose, R. Langer, J. C. Weaver, *Proc. Natl. Acad. Sci. U.S.A.* **90**, 10504 (1993).
6. K. A. Walters, in (*4*), pp. 197–233.
7. J. Kost and R. Langer, in *Topical Drug Bioavailability Bioequivalence and Penetration*, H. I. Maibach and V. P. Shah, Eds. (Plenum, New York, 1993), pp. 91–103.
8. J. Newman, M. D. Nellermore, J. L. Carnett, *J. Am. Podiatr. Med. Assoc.* **82**, 432 (1992).
9. D. M. Skaun and G. M. Zenter, *Int. J. Pharm.* **20**, 235 (1984).
10. W. S. Quillen, *Athl. Train.* **15**, 109 (1980).
11. K. Tachibana, *Pharm. Res.* **9**, 952 (1992).
12. S. Mitragotri, D. Edwards, D. Blankschtein, R. Langer, *J. Pharm. Sci.* **84**, 697 (1995).
13. W. Gaertner, *J. Acoust. Soc. Am.* **26**, 977 (1954).
14. We measured the electrical resistance of the skin prior to each sonophoresis experiment to ensure that the epidermis was not damaged. The epidermis is considered to be damaged if the initial specific epidermis resistance is less than 10 kilohm-cm^2 [J. Rossel, J. Colominas, P. Riu, R. Pallas-Arery, J. Webster, *IEEE Trans. Biomed. Eng.* **35**, 649 (1988)].
15. A Franz diffusion cell (Crown Glass, Somerville, NJ) consists of two compartments, a donor and a receiver compartment. The human cadaver epidermis (separated from the dermis by heat treatment) is mounted between the two compartments and is supported by a Nylon mesh (Tetko, New York) to avoid any damage.
16. The ultrasound intensity, I (spatial average temporal peak), was calculated from the values of the acoustic pressure amplitude, P, measured with a hydrophone (Bruel and Kjaer), by the equation $I = P^2/2\rho c$, where ρ is the water density (1 g/ml) and c is the velocity of ultrasound in water (1500 m/s).
17. The insulin concentration in the receiver compartment was measured every hour by RIA (performed at Linco Research, St. Charles, Montana). We measured the IFN-γ concentration by ELISA (Endogen), and the erythropoeitin concentration was measured by ELISA at Associated and Regional University Pathologists (Salt Lake City, UT).
18. The transdermal flux can be calculated by use of the equation $J = \Delta M/\Delta t$, where ΔM is the amount of protein transported per unit skin area during time Δt. The skin permeability, P, can be calculated from the transdermal flux, J, during the first hour of ultrasound application with the equation $P = J/\Delta C$, where ΔC is the concentration difference across the skin.
19. A typical diabetic patient (70 kg weight) takes ~12 U of insulin three times a day (total dose ~36 U/day) [in *World Book of Diabetes in Practice*, L. P. Krall, Ed. (Elsvier, New York, 1988), pp. 160–163]. If each insulin dose was to be delivered by sonophoresis in 1 hour, the required transdermal flux would be 12 U/hour. One unit of insulin corresponds to ~40 μg.
20. The transdermal patch area used in these calculations was 40 cm^2 [the area of a transdermal Fentanyl patch (Alza)]. The donor concentrations used in these calculations were as follows: insulin, 100 U/ml (Humulin Regular, Eli Lilly); IFN-γ, 3×10^7 U/ml (typical concentration of IFN solution recommended by Genzyme); and erythropoeitin (Amgen), 3×10^5 U/ml [J. Davis, T. Arakawa, T. Strickland, D. Yphantis, *Biochemistry* **26**, 2633 (1987)].
21. A typical IFN-γ dose administered to patients suffering from cancer or viral infection is ~5×10^6 U [J. W. Grups and H. G. Frohmuller, *Br. J. Med.* **64** (no. 3), 218 (1989); J. M. Parkin, L. Eales, A. Galazka, A. Pinching, *Br. Med. J.* **294**, 1185 (1987)]. Similar doses of IFN-α and -β have also been shown to enhance the immune response of these patients [in *Clinical Applications of Interferons and their Inducers*, D. Stringfellow, Ed. (Dekker, New York, 1986), pp. 1–30]. If this IFN dose was to be given by sonophoresis in 1 hour, the required transdermal flux would be 5×10^6 U/hour. One unit of IFN-γ corresponds to ~1 pg.

22. A typical daily erythropoeitin dose given subcutaneously to anemic patients is about 400 U [J. Bommer, E. Ritz, T. Weinreich, G. Bommer, T. Ziegler, *Lancet* **ii**, 406 (1988)]. If this dose was to be delivered in three steps, each involving sonophoresis for 1 hour, the transdermal flux required would be about 140 U/hour. One unit of erythropoeitin corresponds to ~7.6 ng.
23. R. E. Apfel, *IEEE Trans. Ultrason. Ferroelectrics Freq. Control* 1986, UFFC-33, 139.
24. Transdermal water transport was measured as in the insulin experiments at an ultrasound intensity of 125 mW/cm^2, except that the donor compartment was filled with a 1 μCi of radiolabeled water (^{3}H) per milliliter of solution. The concentration of water in the receiver compartment was measured by means of a scintillation counter. The permeability was calculated by the methods described in (*18*).
25. The transport properties of hairless rat and hairless mouse skin have been shown to resemble those of human skin. The passive permeability of the hairless rat skin to many compounds is within a factor of 2 to 5 of the human skin permeability. [Y. Morimoto, T. Hatanaka, K. Sugibayashi, H. Omiya, *J. Pharm. Pharmacol.* **44**, 634 (1992); R. Wester and H. I. Maibach, in (*7*), pp. 333–347.]
26. The histological studies of the hairless rat skin exposed to ultrasound were performed at Deborah Heart and Lung Institute, NJ. The skin samples exposed to ultrasound, as well as those not exposed to ultrasound (controls), were stained with hematoxylin and eosin. The samples were later observed under a light microscope (40-fold magnification) to be assessed for possible structural damage. Five control skin samples and 20 skin samples exposed to ultrasound (five samples measured at each ultrasound intensity in the range of 12.5 to 225 mW/cm^2) were analyzed.
27. A. D. Walmsley, *Ultrasound Med. Biol.* **14**, (1988).
28. Commercially available portable ultrasound toothbrushes make use of a small sonicator contained within the toothbrush (Sonex International Corporation, Brewster, New York). This sonicator is portable and operates on rechargeable batteries. Modifications of such a system might eventually be used for transdermal application.
29. M. V. Pishko, M. C. Adrian, A. Heller, *Anal. Chem.* **63**, 2268 (1991).
30. All animal procedures were in accordance with approved institutional protocols. The hairless rats were anesthetized with a mixture of ketamine (60 mg/kg) and xylazine (10 mg/kg). After about an hour, a flanged glass cylinder (Crown Glass; diameter, 20 mm; height, 2 cm) was glued onto the back of each rat with a minimal amount of superglue (Permabond, Englewood, NJ) or vacuum grease (Dow Chemicals) on the outer edge of the flange. The center of the cylinder was located about 3 cm from the rear end of the rat. This particular site was chosen so that application of ultrasound directly on a sharp bone close to the body surface was avoided, which otherwise could cause a damage to the blood capillaries near the edge of the bone. This could be especially relevant in the case of young rats (<6 weeks old) because these rats have bones close to the skin surface. The cylinder was filled with an insulin solution (100 U/ml). Ultrasound (20 kHz, 100-ms pulse applied every second) at different intensities was applied by immersion of the transducer (VCX 400, Sonics and Materials) in the insulin solution about 1 cm away from the skin. Duplicate samples of the blood glucose concentration in the tail-vein blood were measured every 30 min with a glucose monitoring device (AccucheckAdvantage, Boeheringer Mannheim).
31. We thank M. Prausnitz for helpful suggestions, S. Liauw and A. Patel for technical assistance, and J. Kost and M. Johnson for helpful discussions. We also thank L. Brown for assistance with diabetic hairless rats, B. Schloo for performing histological studies, and R. Gingerich for assistance with insulin measurements. Supported by NIH grant GM44884 and a gift from the Zachary Miller Fund to R.L., and a fellowship from Schering-Plough Foundation. D.B. acknowledges the support of a NSF Presidential Young Investigator Award.

18 January 1995; accepted 5 June 1995

Parietal Contributions to Visual Feature Binding: Evidence from a Patient with Bilateral Lesions

Stacia R. Friedman-Hill,* Lynn C. Robertson, Anne Treisman

Neurophysiologists have documented the existence of multiple cortical areas responsive to different visual features. This modular organization has sparked theoretical interest in how the "binding problem" is solved. Recent data from a neurological patient (R.M.) with bilateral parietal-occipital lesions demonstrates that the binding problem is not just a hypothetical construct; it can be a practical problem, as rare as the selective inability to perceive motion or color. R.M. miscombines colors and shapes even under free viewing conditions and is unable to judge either relative or absolute visual locations. The evidence suggests that a single explanation—an inadequate spatial representation—can account for R.M.'s spatial judgment and feature-binding deficits.

A perplexing question in vision research is how the brain solves the "binding problem." Primate brains contain more than 20 visual areas, many of which are highly specialized for processing specific visual features (*1*). Data from human and nonhuman subjects demonstrate that object features such as color or shape are represented in hierarchical interconnected areas in a ventral visual pathway that extends from the occipital to the temporal cortex, whereas spatial features are represented in a dorsal pathway from the occipital to the parietal cortex (*2*). The wide cortical distribution of visual features, the large receptive fields of inferotemporal neurons, and the separation of spatial and object pathways lead to the question of how unified perception (or "binding") of visual objects results (*3*). Several neurophysiological studies have proposed temporally correlated neuronal activity as a mechanism for intra- and interareal coordination (*4*). Although research in cats and monkeys has been directed at exploring the neural substrate of binding, there are no documented cases of animals with binding deficits.

Treisman and Gelade (*5*) proposed that attention to spatial locations in normal human brains was necessary to properly bind the features of objects. Feature binding should therefore be disrupted by attentional overload or inaccurate spatial information. The effects of divided or reduced attention have been tested in neurologically normal people and in patient populations (*6*, *7*). When presented with brief displays of colored letters and asked to report the identity of a simultaneously presented digit, subjects experienced illusory conjunctions (ICs), as predicted. For example, if presented with a red X and a blue O, subjects sometimes confidently reported seeing a red O or a blue X. Patients with unilateral neural damage have exhibited an attentional bias away from objects in the contralesional field and have been shown to make more ICs in the contralesional than in the ipsilesional field when stimuli were briefly presented (*7*).

The binding problem seldom poses a serious challenge in nonlaboratory environments. Intact primate brains are so adept at solving the binding problem that severe limitations on processing must be imposed to observe ICs: ICs are seen in normal people only when attentional demands are high and displays are brief (200 ms) or peripheral (*6*, *8*). We have been testing, with informed consent, a 58-year-old patient (R.M.) for whom the binding problem is a significant practical challenge. R.M. has nearly symmetrical bilateral parieto-occipital lesions (Fig. 1, A to C) (*9*), with no temporal or frontal lobe involvement. R.M. did not exhibit an attentional bias for the left or right visual field but did have great difficulty in reporting where objects were located even when he directed his gaze at them. We could therefore investigate the effects of degraded spatial information on feature binding. We assessed R.M.'s ability to properly conjoin features by presenting displays containing two colored letters. His task was to report the name and color of the first letter he saw (*10*). R.M. had an IC rate of 13% even when display times were as long as 10 s and even when his attention was undivided (Fig. 2). In earlier testing sessions, his error rate was 25%, but no

S. R. Friedman-Hill, Center for Neuroscience, University of California, Davis, CA 95616, USA.
L. C. Robertson, Veterans Administration and Center for Neuroscience, University of California, Davis, CA 95616, USA.
A. Treisman, Department of Psychology, Princeton University, Princeton, NJ 08540, USA.
*To whom correspondence should be addressed.